ELSEVIER

PII: S0021-9290(97)00015-8

J. Biomechanics, Vol. 30, No. 7, pp. 705–712, 1997

Printed in Great Britain
0021-9290/97 $17.00 + .00

HOW MUSCLE ARCHITECTURE AND MOMENT ARMS AFFECT WRIST FLEXION-EXTENSION MOMENTS

Roger V. Gonzalez,* Thomas S. Buchanan† and Scott L. Delp

Departments of Biomedical Engineering and Physical Medicine & Rehabilitation, Northwestern University and Sensory Motor Performance Program, Rehabilitation Institute of Chicago, Room 1406, 345 East Superior St., Chicago, IL 60611, U.S.A.; *Mechanical Engineering Department, Le Tourneau University, Longview, TX 75607, U.S.A.; and †Mechanical Engineering Department, University of Delaware, Newark, DE 19716, U.S.A.

Abstract—The purpose of this investigation was to determine how the moment arms and architecture of the wrist muscles influence their isometric moment-generating characteristics. A three-dimensional computer graphics model was developed that estimates the moment arms, maximum isometric forces, and maximum isometric flexion–extension moments generated by 15 muscles about the wrist over a range of wrist flexion angles. In combination with measurements of muscle strength, we used this model to answer three questions: (1) why is peak wrist flexion moment greater than peak extension moment, (2) why does flexion moment vary more with wrist flexion angle than does extension moment, and (3) why does flexion moment peak with the wrist in a flexed position? Analysis of the model revealed that the peak flexion moment is greater than the peak extension moment primarily because of the larger (110%) summed physiologic cross-sectional area of the flexors. The larger variation of flexion moment with flexion angle is caused mainly by greater variation of the moment arms of the major wrist flexors with flexion angle. The location of the peak flexion moment is determined by the wrist flexion moment arms (which tend to increase with wrist flexion) in combination with the force–length characteristics of these muscles.

Keywords: Wrist; Muscle architecture; Moment arms.

INTRODUCTION

Measuring the moments generated by muscles under conditions of maximum voluntary contraction is the most common method used to assess muscle strength in general (Kulig *et al.*, 1984) and at the wrist in particular (Jacobson *et al.*, 1992; Ketchum *et al.*, 1978; Lehman and Calhoun, 1990). We recently reported maximum isometric wrist moments generated by ten healthy subjects over a range of wrist flexion angle (Delp *et al.*, 1996). These measurements revealed three important features of the wrist muscles. First, the peak moment generated by the wrist flexors was substantially greater than the peak moment generated by the extensors. Second, the maximum flexion moment generated by the subjects varied more with wrist flexion angle than did the maximum extension moment. Third, the peak flexion moment occurred with the wrist in a flexed position, where the muscle fibers are relatively short. Although these findings represent a first step in characterizing the normal function of wrist muscles, the experimental data alone do not allow one to determine how muscle architecture (arrangement and length of muscle fibers) and moment arms influence the moment-generating characteristics of the wrist muscles.

Several factors contribute to the maximum isometric moment generated by an individual muscle, including its physiologic cross-sectional area (PCSA), moment arm (MA), and activation. Other factors contribute to the change in the isometric moment with joint angle, such as variation of MA with joint angle and the muscle's force–length behavior. Thus, the three experimental observations cited above could be explained by a number of different mechanisms. For example, the peak flexion moment would be larger than peak extension moment if the MAs of the flexors were greater than the MAs of the extensors and/or the total PCSA of the flexors were larger than the PCSA of the extensors. The greater variation of flexion moment with joint angle could also arise from several mechanisms, including a greater variation of flexor MAs with wrist angle and/or a smaller ratio of optimal muscle-fiber length to MA for the flexors, which causes a larger variation of sarcomere length with joint angle (Delp and Zajac, 1992; Lieber and Bodine-Fowler, 1993). The occurrence of the peak flexion moment in a flexed wrist position could arise from (1) the positions of the peak MAs of the major wrist flexors, (2) the positions of the peak forces generated by the major wrist flexors, or (3) a combination of force and moment arm variation with wrist flexion.

The purpose of this work was to investigate how the moment arms and architecture of the wrist muscles contribute to their moment-generating characteristics. The investigation was organized around three hypotheses. First, we hypothesized that the peak flexion moment was greater than the peak extension moment because the sum of the PCSA-MA products is greater for wrist flexors than for the extensors. Second, we hypothesized that the greater variation of flexion moment with wrist angle was due to the larger variation of flexor MAs with joint angle. Third, we hypothesized that flexion moment peaked with the wrist in flexion because of a combination of force and moment arm variation with wrist flexion.

Because there are a large number of muscles that span the wrist, a biomechanical model is needed to analyze the

Received in final form 6 *January* 1997.
Address correspondence to: Scott L. Delp, Sensory Motor Performance Program, Rehabilitation Institute of Chicago, Rm. 1406, 345 East Superior St., Chicago, IL 60611, U.S.A.

contributions of the muscle moment arms and architecture to the moment-generating capacity. Although several investigators have developed models of the upper limb (Buchanan *et al.*, 1993; Gonzalez *et al.*, 1996; Loren *et al.*, 1996; Raikova, 1992; Winters and Kleweno, 1993; Yamaguchi *et al.*, 1995), none have developed a model of the human wrist that includes all the muscles that span the joint. Therefore, we developed, tested, and analyzed a detailed biomechanical model of the wrist muscles to determine how their PCSAs, fiber-operating lengths, and moment arms influence wrist muscle strength.

METHODS

The wrist model represents the three-dimensional geometry of the bones, kinematics of the joints, and the lines of action and force-generating properties of 15 muscles. These muscles are: abductor pollicis longus (APL), extensor carpi radialis brevis (ECRB), extensor carpi radialis longus (ECRL), extensor carpi ulnaris (ECU), extensor digitorum communis (EDC), extensor digiti minimi (EDM), extensor indicis proprius (EIP), extensor pollicis brevis (EPB), extensor pollicis longus (EPL), flexor carpi radialis (FCR), flexor carpi ulnaris (FCU), flexor pollicis longus (FPL), flexor digitorum profundus (FDP), flexor digitorum superficialis (FDS), and palmaris longus (PL). Muscles EDC, FDP, and FDS were each represented by four digital units corresponding to the index (I), middle (M), ring (R), and little (L) fingers (Fig. 1).

The wrist model was implemented using the musculoskeletal modeling software (SIMM) described by Delp and Loan (1995) and Delp *et al.* (1990). The bone geometry was obtained by digitizing the humerus, ulna, radius, carpals, and metacarpals from a male skeleton with the use of an instrumented linkage (Faro Technologies Inc.). The muscle origins, insertions, and paths were defined based on anatomical landmarks of the bone surfaces. In addition to the muscle origins and insertions, intermediate points were introduced to constrain the muscle paths to wrap over bones, to simulate the constraints imposed by retinacula, and to assure anatomical accuracy of the model.

Wrist kinematics were constrained to the planar motion of wrist flexion–extension. The kinematics of flexion–extension were represented as two revolutes to account for motion of the radiocarpal and midcarpal joints (Ruby *et al.*, 1988). The approximate axes of rotation were at the center of the lunate for the radiocarpal joint and at the center of the capitate for the midcarpal joint. Wrist flexion–extension was distributed evenly between the two joints. For example, a 70° flexion of the wrist was accomplished by a 35° rotation about the radiocarpal joint axis and a 35° rotation about the midcarpal joints axis. In the model, there was no motion of the individual carpals within a carpal row and no radial or ulnar deviation (i.e. third digit was aligned with the long axis of the forearm). The carpometacarpal joints and interphalangeal joints remained at full extension during wrist flexion–extension, as shown in Fig. 1. Although the position of the fingers can be altered in the model, the finger positions were fixed in this analysis so that muscle length changes resulted exclusively from motion of the wrist. The range of motion of the wrist model was limited to 70° extension and 70° flexion.

The isometric force-generating property of each muscle was derived by scaling a Hill-type muscle model (Delp and Loan, 1995; Zajac, 1989). Four parameters scaled the generic force–length curves for muscle and tendon (Fig. 2) to represent an individual muscle–tendon complex. The four parameters were: peak isometric force (F_o^m), optimal muscle fiber length (l_o^m), pennation angle (α^m), and tendon slack length (l_s^t). Three of the four parameters (F_o^m, l_o^m, α^m), were derived directly from anatomical experiments. Values for l_o^m, and α^m were taken from detailed reports of muscle architecture (Jacobson *et al.*, 1992; Lieber *et al.*, 1990, 1992); all the reported

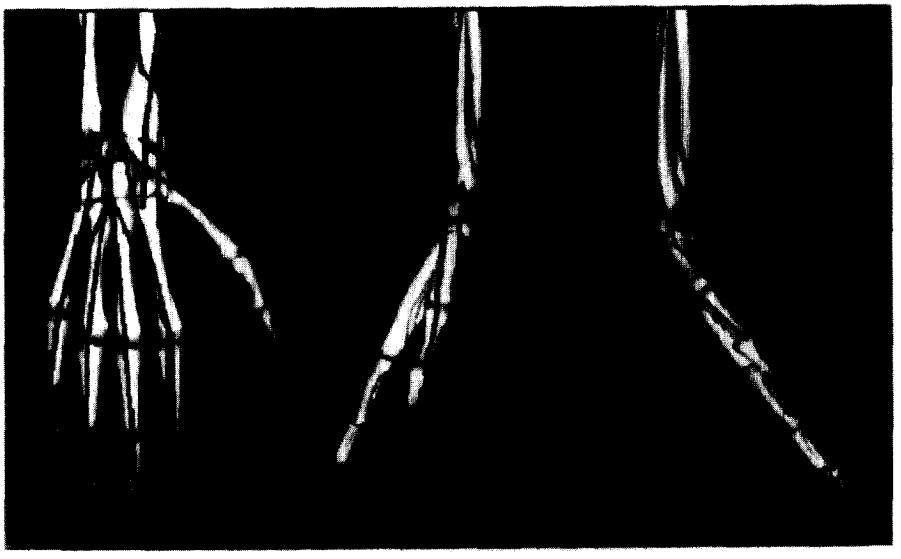

Fig. 1. Muscle–tendon paths with the wrist in neutral (left, dorsal view), extended (center), and flexed (right) positions.

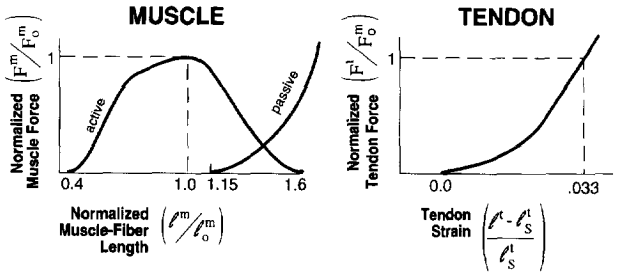

Fig. 2. Generic muscle and tendon force-length curves used in the wrist model. Muscle force is assumed to be the sum of muscle force when it is inactive (passive) and when it is maximally excited (active). The forces in muscle (F^m) and tendon (F^t) are normalized by peak isometric muscle force (F_o^m). Muscle-fiber length (l^m) is normalized by optimal muscle-fiber length (l_o^m). Tendon slack length (l_s^t) is the length of tendon at which force begins to develop.

optimal fiber lengths were multiplied by a correction factor of 2.7/2.2 to account for the difference between the optimal sarcomere length of mammalian muscle (2.7 μm, Woledge *et al.*, 1985) and the optimal sarcomere length of amphibian muscle used in the previous publications (2.2 μm). Peak isometric forces, F_o^m, were determined from anatomical measurements of the PCSA of each muscle (Jacobson *et al.*, 1992; Lieber *et al.*, 1990, 1992). Different factors were used to linearly scale PCSA to F_o^m for the flexors (30 N cm^{-2}) and extensors (45 N cm^{-2}). These factors were derived by comparing the experimentally measured maximum isometric joint moments computed with the model to the maximum moments reported by Delp *et al.* (1996). Buchanan (1995) showed that it is often necessary to use different values of maximum muscle stress for different muscle groups when scaling PCSAs from cadaver data. Tendon slack lengths, l_s^t, were set such that the passive moments (i.e. the moments generated by the muscles when they are inactive) computed with the model were consistent with experimentally measured passive wrist moments (Delp *et al.*, 1996).

The model was used to calculate muscle moment arms, maximum isometric forces, and maximum isometric moments from 70° extension to 70° flexion. Muscle MAs were determined by calculating the change in the muscle–tendon length (∂l^{mt}) with respect to the change in wrist flexion angle ($\partial\theta$) (An *et al.*, 1984; Brand *et al.*, 1975; Delp and Loan, 1995; Storace and Wolf, 1979):

$$\mathrm{MA} = \frac{\partial l^{mt}}{\partial \theta} \quad (1)$$

The maximum isometric force generated by a muscle over a range of flexion angle was determined by assuming the muscle was maximally activated and calculating the force (active plus passive) corresponding to each flexion angle (i.e. muscle–tendon length). The maximum isometric moment generated by each muscle was calculated as the product of the muscle's maximum isometric force vs flexion angle curve and its MA vs flexion angle curve. The moments generated by all of the flexors were summed to produce the total isometric flexion moment. Maximum isometric extension moments were calculated with the same procedure.

Using the MAs estimated with the model, the sum of the PCSA-MA products were calculated for the flexors and extensors. These calculations were made in the neutral wrist position (0° flexion) and at the joint angles corresponding to the peak flexion and extension moments. To assure that these products were evaluated accurately, the MA values estimated with the computer model were compared to the experimental data from Brand and Hollister (1993) and Loren *et al.* (1996). After the model's MAs and maximum moment estimations were verified with experimental data, the model was used to analyze how the muscle MAs and architectures contributed to the observed moments. The results below provide an evaluation of the model followed by a test of each hypothesis stated in the Introduction.

RESULTS

The moment arms calculated with the model at the neutral wrist position correspond well with MAs reported by Brand and Hollister (1993) and Loren *et al.* (1996) (Fig. 3). The model's MA–joint angle relationship for the five dedicated wrist muscles (i.e. muscles that cross the wrist but do not cross the interphalangeal joints) also approximate the experimental data of Loren *et al.* (1996) (Fig. 4). Specifically, the moment arms estimated for the FCR and FCU closely match the experimental data throughout the range of motion. The model and the experimental data also demonstrate the same relative magnitudes of the extensor moment arms. However, the variation of the extensor moment arms with flexion angle differs between the computer model and the experimental results. The moment arms calculated for FDS and FDP correspond well with moment arms reported by Brand and Hollister (Fig. 5). The model and experimental data show large changes in the MA magnitude between $\pm$ 20°. MA-angle estimations determined by the model for the remaining wrist muscles are shown in the appendix.

The operating ranges of the five dedicated wrist muscles are similar to ranges reported by Loren *et al.* (1996) (Fig. 6). The model matches the experimental data, except the FCR muscle, which operates at longer lengths in the model. The model was not adjusted to match the fiber operating range measurements of Loren *et al.*; these data were used only for comparison with the model.

The model reproduces the three findings in the experimentally measured maximal isometric wrist flexion and extension moments (Fig. 7). First, peak flexion moment is approximately 70% greater than peak extension moment in both the computer model and the experimental results. Second, flexion moment varies with flexion angle by approximately 6 N m (57%) while extension moment varies approximately 2.5 N m (38%). Third, the flexion moment peaks in a slightly flexed wrist position. The largest differences between the model and the experimental results occur with the wrist in full extension (−70°). The extension moment calculated with the model was 1.5 N m less than the measured moment at full extension, and the flexion moment calculated by the model was 1.9 N m larger than the measured flexion moment.

The sum of the PCSA-MA products was greater for the flexors than for the extensors; this explains the

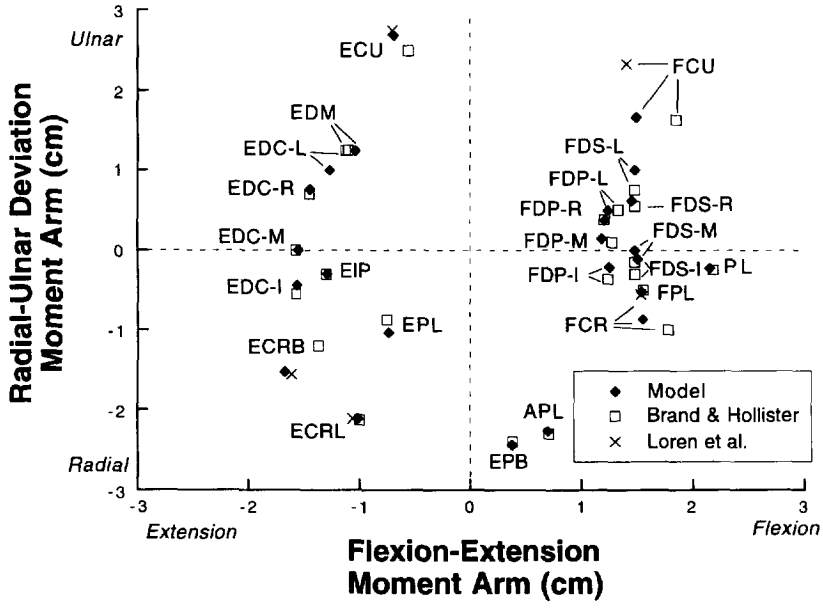

Fig. 3. Comparison of model moment arms to experimentally determined moment arms at neutral wrist flexion–extension and radial–ulnar deviation. Extension and radial deviation are negative, flexion and ulnar deviation are positive. Moment arms in flexion–extension and radial–ulnar deviation agreed well to those defined by Brand and Hollister (1993) and Loren *et al.* (1996) at the neutral position, except for the ECRB, ECU, FCR, and FCU where the model moment arms had a value intermediate to those reported by the two investigations. See Methods for muscle abbreviations.

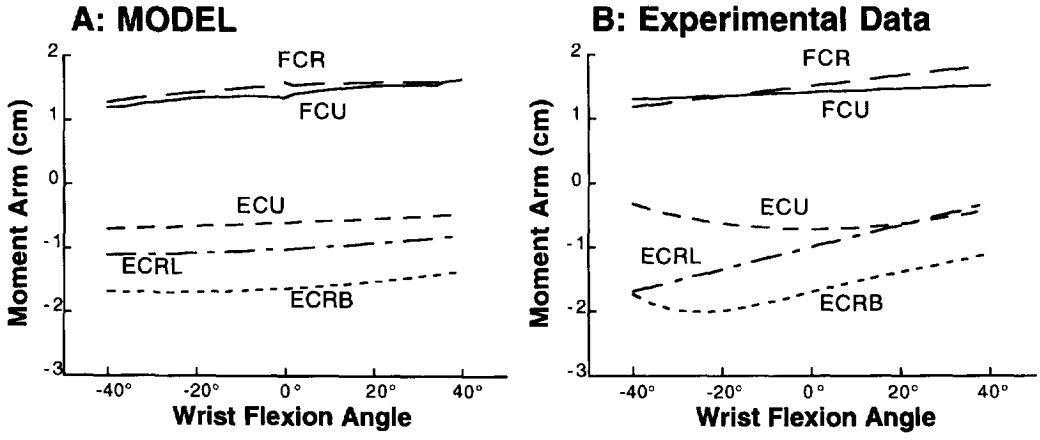

Fig. 4. Flexion–extension moment arms from the model (A) and Loren *et al.* (1996) (B). Moment arms are negative for extensor muscles and positive for flexor muscles. The experimental MA–angle relations were derived by using a stepwise polynomial regression of multiple wrist muscle samples as described by Loren *et al.*, (1996). See Methods for muscle abbreviations. Flexion angles are positive, extension angles are negative.

experimental observation that the flexors are capable of generating a larger peak moment than the extensors. In the neutral wrist position, the sum of the PCSA-MA products is 32 cm^3 for the flexors and 14 cm^3 for the extensors (Table 1). At the joint angles corresponding to the peak moments (40° for flexors and −20° for extensors), the sum of the PCSA-MA products is 44 cm^3 for the flexors and 15 cm^3 for the extensors. The flexors have approximately twice the total PCSA as the extensors; this is the primary factor that accounts for their greater moment-generating capacity. At the joint angles corresponding to the peak moments, the average flexor moment arm is 23% larger than the average extensor moment arm; this is the secondary factor that accounts for the peak flexion moment being larger than the peak extension moment.

Two factors lead to the greater variation of flexion moment with flexion angle. First, and more importantly, the moment arms of the flexors vary more with flexion angle. Between the angles of minimum and maximum moments, the flexor MAs vary 45% from their maximum values, on average, while the extensor MAs vary 34%. Second, the force-generating capacities of the flexors vary more with joint angle than the extensors. Averaged between the

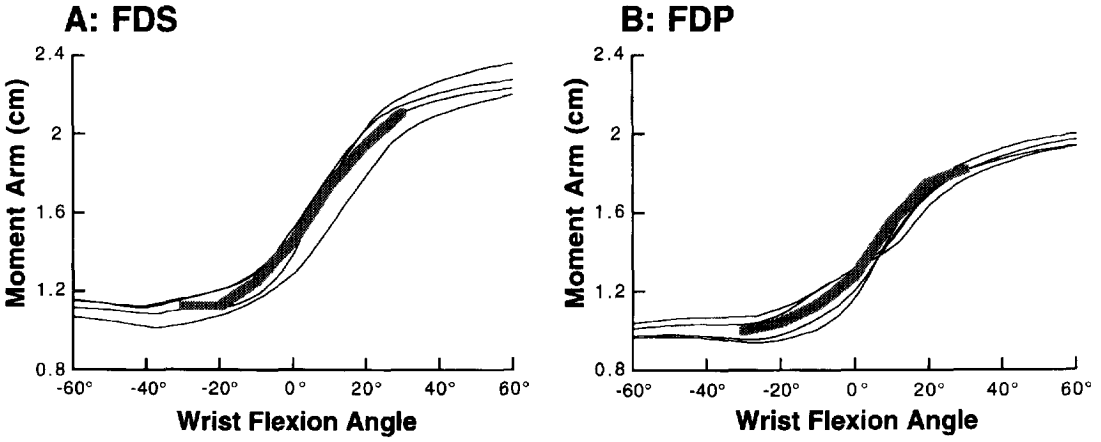

Fig. 5. Moment arms for FDS (A) and FDP (B) from the model and experimental results. The moment arms estimated for each of the four digital units shown in Fig. 1 (thin curves) are compared to the moment arm (thick curve) approximated from Brand and Hollister (1993). See Methods for muscle abbreviations. Flexion angles are positive, extension angles are negative. Note that the moment arms increase with flexion.

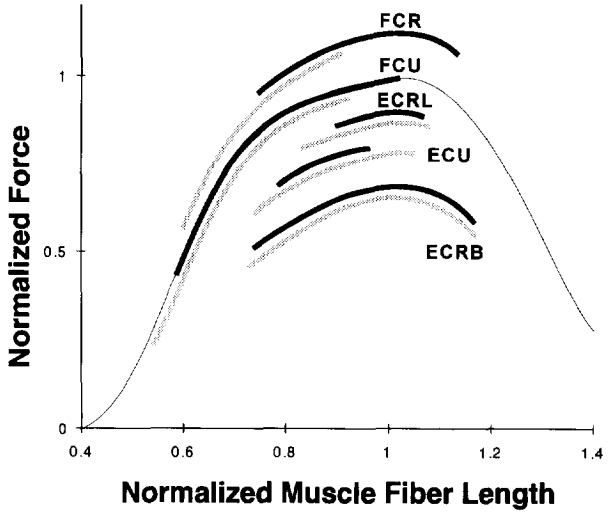

Fig. 6. Operating lengths of five wrist muscles from 50° flexion to 45° extension. Values approximated from Loren *et al.* (1996) for the same range of motion are the shaded curves. Model results are the dark curves. The thin line represents the entire force–length relation of muscle.

wrist angles of minimum and maximum moments, the flexor muscle forces vary 14% from their maximum values, on average, while the extensors muscle forces vary only 8%, on average. Although the average value of the ratio of optimal fiber length to average moment arm (l_o^m/MA^{Ave}) is similar for the flexors and extensors (Table 1), when only the top four potential contributors to flexion (FDP, FDS, FCU, FPL) and extension (EDC, ECRB, ECU, ECRL) moments are considered, the average l_o^m/MA^{Ave} is smaller for the flexors than extensors (4.3 vs 7.2); this smaller ratio for the flexors leads to greater variation of sarcomere length with flexion angle.

Flexion moment peaks in a slightly flexed position because the moment arms of several important wrist flexors (FDP, FDS, FCR, FCU) increase as the wrist is flexed. As long as the force-generating capacity of these muscles remains relatively constant (i.e. while the muscles operate on the plateau region of the force–length curve) moment increases with flexion. However, as the wrist flexes, the muscle fibers become short and reach the ascending region of the force–length curve. The increasing moment arm and the decreasing force determine the position of the peak moment of one of the dedicated flexors, FCU (Fig. 8A), and of the flexor group (Fig. 8B).

The digital flexors and extensors contribute substantially to wrist moment generating potential. For example, at the joint angle of peak flexion moment (40°), FDS and FDP account for 68% of the total moment-generating capacity of the flexors, whereas the dedicated wrist flexors (FCU, FCR) provide only 16% of the total (the remaining flexor muscles, FPL, APL, PL, and EPB account for 16%). Similarly, at the angle of peak extension moment (−20°), EDC, EDM, EPL, and EIP produce 45% of the total extension moment potential, whereas the dedicated wrist extensors (ECU, ECRB, ECRL) provide 55% of the total.

DISCUSSION

The purpose of this study was to examine how the moment arms and architectures of the muscles contribute to observed maximum isometric flexion and extension moments about the wrist. The biomechanical model of the wrist presented here replicated the experimental flexion and extension moments reported by Delp *et al.* (1996). Analysis of the model demonstrated that the variations of the maximum isometric moments with flexion angle are critically dependent on variation of the moment arms with flexion angle and the operating lengths of the muscles fibers.

Several assumptions and limitations of this study should be considered. First, even though the computer model replicates the measured joint moments reasonably well, it is difficult to have full confidence in the individual muscle force estimates because many muscles contribute to the measured moments. Fortunately, excellent measurements of muscle architecture (Lieber *et al.*, 1992;

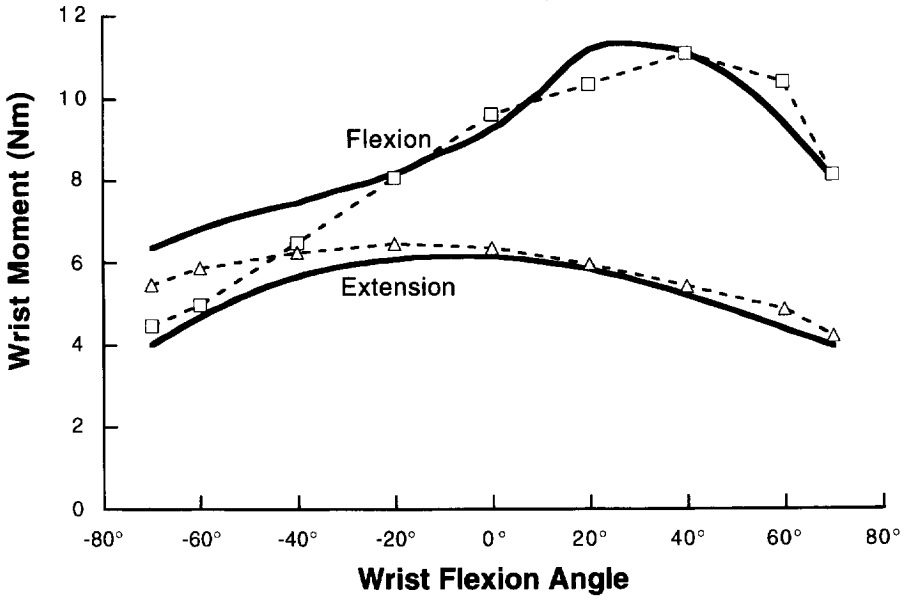

Fig. 7. Maximum isometric flexion and extension moments vs wrist joint angle. The squares and triangles represent the mean of ten subjects (Delp *et al.*, 1996). The solid curves represent the maximum isometric moments calculated with the model. Flexion angles are positive, extension angles are negative. The mean flexion moment peaked at approximately 40°; the extension moment peaked at −20°, and varied less with wrist flexion angle.

Table 1. Flexor and extensor parameter values used by the model and muscle forces and moment arms estimated by the model. Physiologic cross-sectional area (PCSA) and optimal muscle fiber length (l_o^m) values were taken from Jacobson *et al.* (1992) and Lieber *et al.* (1990, 1992). Peak isometric muscle force (F_o^m) was calculated based on PCSA (see Methods). Moment arms (MAs) were estimated at the neutral position (0°) and the positions of peak moments: 40° for the flexors and −20° for the extensors. The PCSA-MA products were calculated for the muscles at these wrist positions. The ratios of l_o^m/MA^{Ave} are also shown, where MA^{Ave} is the average value of the MA between ± 70°. Muscle force is in Newtons (N). MAs and l_o^m are in centimeters (cm) and PCSAs are in (cm^2). See Methods for muscle abbreviations

Flexors	PCSA	F_o^m	l_o^m	Muscle force at Neutral	MA at neutral		MA at 40°		l_o^m/MA^{Ave}
					(MA^n)	PCSA * MA^n	(MA^{40})	PCSA * MA^{40}	
FDP	7.9	238	7.8	234	1.2	9.4	1.8	14.3	5.8
FDS	6.3	188	7.1	182	1.4	8.6	2.2	13.7	4.4
FCU	3.4	103	5.1	90	1.4	4.7	1.6	5.6	3.6
FPL	2.1	62	5.5	62	1.4	2.8	2.1	4.3	3.4
FCR	2.0	60	6.3	59	1.6	3.2	1.6	3.2	4.4
PL	0.7	21	6.4	21	2.1	1.5	2.3	1.6	3.1
APL	1.9	58	7.1	55	0.8	1.5	0.7	1.4	10.0
EPB	0.5	14	6.8	13	0.4	0.2	0.4	0.2	17.5
Average					1.3		1.6		6.5
Sum	24.8					31.8		44.3	

Extensors	PCSA	F_o^m	l_o^m	Muscle force at Neutral	MA at neutral		MA at −20°		l_o^m/MA^{Ave}
					(MA^n)	PCSA * MA^n	(MA^{-20})	PCSA * MA^{-20}	
EDC	2.8	126	6.8	113	1.6	4.5	1.7	4.7	4.2
ECRB	2.7	123	5.9	120	1.6	4.4	1.7	4.6	3.9
ECU	2.6	117	6.2	111	0.6	1.5	0.7	1.7	10.8
ECRL	1.5	66	9.4	66	1.0	1.5	1.1	1.6	9.9
EDM	0.6	29	6.6	28	1.5	0.9	1.5	1.0	4.6
EPL	1.0	44	5.4	43	0.8	0.8	0.8	0.8	7.2
EIP	0.6	25	5.9	23	1.3	0.8	1.4	0.8	4.5
Average					1.2		1.3		6.5
Sum	11.8					14.5		15.2	

Loren *et al.*, 1996) and detailed reports of muscle moment arms (Brand and Hollister, 1993; Loren *et al.*, 1996) are available to test the model. Our model produces fiber-operating ranges and moment arms that are consistent with these experimental data. However, additional measurements of muscle-fiber-operating ranges are needed for FDS, FDP, and EDC to further test the computer model. This is especially important considering

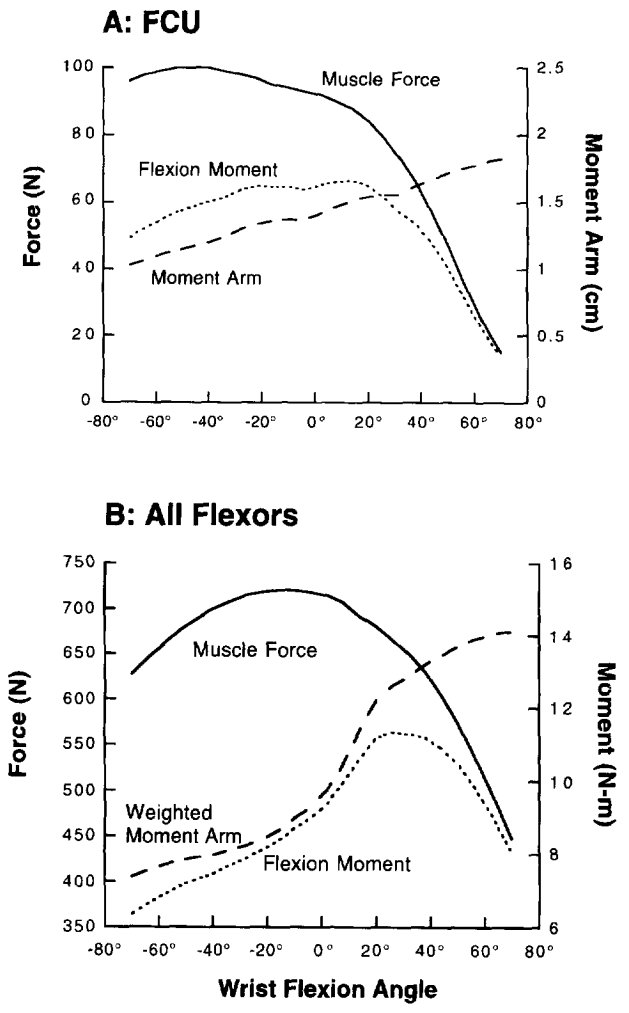

Fig. 8. Maximum isometric force, moment arm, and flexion moment vs flexion angle. In A, the solid curve is the maximum isometric force generated by the flexor carpi ulnaris, FCU, the dashed curve is moment arm (as shown in Fig. 4), and dotted curve is flexion moment (the peak moment is 1.3 N m). In B, the solid curve represents the sum of the forces generated by all of the flexors, the dashed curve is the sum of the MA-F_0^m products for the flexors, and is labeled 'weighted moment arm'. Flexion angles are positive, extension angles are negative. Note that the positions of the peak moments result from the interplay of moment arm–angle and force-angle relations.

the potentially large contributions these muscles make to flexion and extension moments about the wrist.

The model assumes constant, maximal activation for each agonist muscle. Also, the model does not require the muscles to be activated such that radial-ulnar deviation and finger moments are zero during a simulated maximum contraction (this is consistent with our experimental protocol that did not require subjects to balance deviation moments or finger moments during maximum voluntary flexion–extension contractions). Therefore, this study did not examine how muscle activation patterns affect the moment-generating characteristics of muscles about the wrist. In our previous experimental study of wrist muscle strength (Delp *et al.*, 1996), analysis of surface EMG recordings demonstrated no significant variations in muscle activity with wrist flexion angle for the range of motion reported here (−70 to 70°). However, there was evidence of co-contraction in some subjects, which was not accounted for in the computer model. Additional experimental studies that measure activity of individual wrist muscles during maximum voluntary contractions are needed to determine how muscle activation patterns affect flexion and extension moments.

Homogeneous muscle fiber lengths and a single optimal fiber length were assumed in the model of each muscle. Brand and Hollister (1993) have described the ECRL as having different fiber lengths depending on the location of the fibers within the muscle, and presumably other muscles have variability in fiber lengths as well. The inclusion of heterogeneous fiber lengths in the model of each muscle would produce a broader force–length curve, and potentially less change in force with flexion angle than the results reported here.

Wrist flexion–extension was divided evenly between the radiocarpal and midcarpal joints in the model, and the kinematics were assumed to be invariant with muscle force. However, other studies have indicated that wrist flexion–extension may produce different magnitudes of rotation at radiocarpal and midcarpal joints (Berger and Crowninshield, 1982; Sennwald *et al.*, 1993) and that the motions of the wrist may be load-dependent (Valero-Cuevas and Small, 1997).

The model reported here represents the geometry of a single specimen and utilizes average muscle–tendon parameters collected in anatomical studies. Although this model represents the average moment-generating characteristics well, individual variations in musculoskeletal geometry and muscle–tendon parameters can influence moment-generating characteristics substantially. Clearly, research aimed at demonstrating how individual variations, including pathologic changes, can be incorporated into musculoskeletal models is an important area for future investigations.

In general, subjects cannot selectively activate their dedicated wrist flexor and extensor muscles during maximal isometric contractions; this makes it difficult to estimate their contribution to the total joint moment experimentally. Analysis of the model presented here indicates that the dedicated wrist flexors (FCU and FCR) provide a relatively small percentage of the total flexion moment-generating potential. This suggests that digital muscles (FDS and FDP) potentially play a major role in producing wrist flexion moments during maximum voluntary contractions.

Our results show that the greater PCSAs of the flexors is the primary reason that the magnitude of the peak flexion moment is greater than the peak extension moment. The larger variation in the flexion moment with joint angle arises primarily from the larger variation of flexor MAs with joint angle. The position of the peak flexion moment is determined by the interplay of the flexor MAs and their force–length behaviors.

We believe that the development of a detailed model of the wrist will help elucidate the factors that contribute to normal muscle function, analyze the causes of deformities that arise in disorders such as rheumatoid arthritis, and help design tendon transfer surgeries and joint replacements to restore musculoskeletal function. The model described here represents a first step in this development.

Acknowledgements— We would like to thank Anita Grierson for the development of a preliminary wrist model, Dr Richard L. Lieber for providing experimental data on wrist muscle moment arms and Scott Riewald for helpful comments on the manuscript. This work is supported by NIH AR40408 and NSF BCS9257299.

REFERENCES

An, K. N., Takahaski, K., Harrigan, T. P. and Chao, E. Y. (1984) Determination of muscle orientations and moment arms. *J. biomech. Engng* **106,** 280–282.

Berger, R. A. and Crowninshield, R. D. (1982) The three-dimensional rotational behaviors of the carpal bones. *Clin. orthop. Rel. Res.* **167,** 303–310.

Brand, P. W., Cranor, K. C. and Ellis, J. C. (1975) Tendon and pulleys at the metacarpophalangeal joint of a finger. *J. Bone Jt. Surg.* **57A,** 779–784.

Brand, P. W. and Hollister, A. (1993) *Clinical Mechanics of the Hand.* Mosby Year Book, Chicago.

Buchanan, T. S. (1995) Evidence that maximum muscle stress is not a constant: differences in specific tension between elbow flexors and extensors. *Med. Engng Phys.* **17,** 529–536.

Buchanan, T. S., Moniz, M. J., Dewald, J. P. A. and Rymer, W. Z. (1993) A biomechanical model of muscle forces about the wrist joint during isometric tasks. *J. Biomechanics* **26,** 547–560.

Delp, S. L., Grierson, A. E. and Buchanan, T. S. (1996) Maximum isometric moments generated by the wrist muscles in flexion–extension and radial-ulnar deviation. *J. Biomechanics* **29,** 1371–1375.

Delp, S. L. and Loan, J. P. (1995) A graphics-based software system to develop and analyze model of musculoskeletal structures. *Comput. Biol. Med.* **25,** 21–34.

Delp, S. L., Loan, J. P., Hoy, M. G., Zajac, F. E., Topp, E. L. and Rosen, J. M. (1990) An interactive graphics-based model of the lower extremity to study orthopaedic surgical procedures. *IEEE Trans. biomed. Engng* **37,** 757–767.

Delp, S. L. and Zajac, F. E. (1992) Force- and moment-generating capacity of lower-extremity muscles before and after tendon lengthening. *Clin. Orthop.* **284,** 247–259.

Gonzalez, R. V., Hutchins, E. L., Barr, R. E. and Abraham, L. D. (1996) Development and evaluation of a musculoskeletal model of the elbow joint complex. *J. biomech. Engng* **118,** 32–40.

Jacobson, M. D., Raab, R. R., Fazeli, B. M., Abrams, R. A., Botte, M. J. and Lieber, R. L. (1992) Architecture design of the human intrinsic hand muscles. *J. Hand Surg.* **17A,** 804–809.

Ketchum, L. D., Brand, P. W., Thompson, D. and Pocock, G. S. (1978) The determination of moments for extension of the wrist generated by muscles of the forearm. *J. Hand Surg.* **3,** 205–210.

Kulig, K., Andrews, J. G. and Hay, J. G. (1984) Human strength curves. *Exer. Sports Sci. Rev.* **12,** 417–466.

Lehman, S. L. and Calhoun, B. M. (1990) An identified model for human wrist movements. *Exp. Brain. Res.* 199–208.

Lieber, R. L. and Bodine-Fowler, S. C. (1993) Skeletal muscle mechanics: implications for rehabilitation. *Phys. Therapy* **73,** 844–856.

Lieber, R. L., Fazeli, B. M. and Botte, M. J. (1990) Architecture of selected wrist flexor and extensor muscles. *J. Hand Surg.* **15A,** 244–250.

Lieber, R. L., Jacobson, M. D., Fazeli, B. M., Abrams, R. A. and Botte, M. J. (1992) Architecture of selected muscles of the arm and forearm: anatomy and implications for tendon transfer. *J. Hand Surg.* **17A,** 787–798.

Loren, G. J., Shoemaker, S. D., Burkholder, T. J., Jacobson, M. D., Friden, J. and Leiber, R. L. (1996) Human wrist motors: biomechanical design and application to tendon transfers. *J. Biomechanics* **29,** 331–342.

Raikova, R. (1992) A general approach for modeling and mathematical investigation of the human upper limb. *J. Biomechanics* **25,** 857–867.

Ruby, L. K., Cooney, W. P., An, K. N., Linscheid, R. L. and Chao, E. Y. S. (1988) Relative motion of selected carpal bones: a kinematic analysis of the normal wrist. *J. Hand Surg.* **13A,** 1–10.

Sennwald, G. R., Zdravkovic, V., Kern, H. P. and Jacob, H. A. (1993) Kinematics of the wrist and its ligaments. *J. Hand Surg.* **18A,** 805–814.

Storace, A. and Wolf, B. (1979) Functional analysis of the role of the finger tendons. *J. Biomechanics* **12,** 575–578.

Valero-Cuevas, F. J. and Small, C. F. (1997) Load dependence in carpal kinematics during wrist flexion *in vivo*, *Clin. Biomech.* **12**(3).

Winters, J. M. and Kleweno, D. G. (1993) Effect of initial upper-limb alignment on muscle contributions to isometric strength curves. *J. Biomechanics* **26,** 143–153.

Woledge, R. C., Curtin, N. A. and Homsher, E. (1985) *Energetic Aspects of Muscle Contraction.* Academic Press, New York, NY.

Yamaguchi, G. T., Moran, D. W. and Si, J. (1995) A computationally efficient method for solving the redundant problem in biomechanics. *J. Biomechanics* **28,** 999–1005.

Zajac, F. E. (1989) Muscle and tendon: properties, models, scaling, and application to biomechanics and motor control. *CRC Crit. Rev. biomed. Engng* **17,** 359–411.

APPENDIX

Moment arms of muscles that have secondary roles at the wrist were estimated by the model (Fig. A1). The palmaris longus and flexor pollicis longus have moment arms that vary substantially with wrist flexion angle. Moment arm–joint angle data for these muscles have not been available previously.

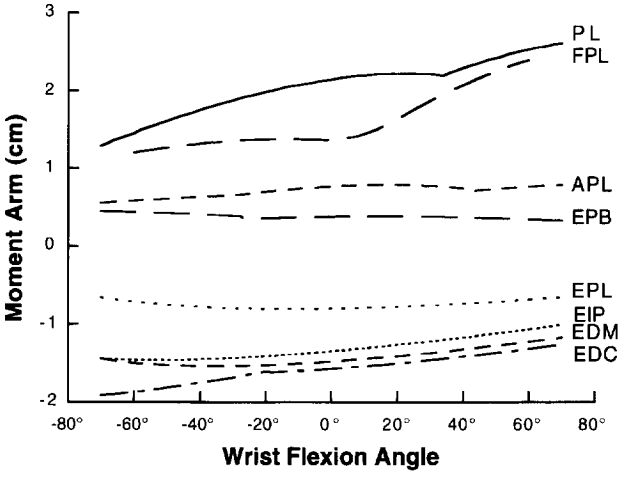

Fig. A1. Wrist muscle moment arms vs wrist flexion angle. Negative moment arms for extensor muscles, positive for flexor muscles. Positive angles are flexion, negative are extension. See Methods for muscle abbreviations.